Investigation of Corrosion Behavior of the AA5754 Aluminum Alloy Joined Using Friction Stir Welding Method

Ferda Mindivan[1], Hasan Kaya[2], Mesut Özer[3], Mehmet Uçar[4], Ramazan Samur[5*]

[1]Department of Technical Programs, Bilecik S.E. University, Bilecik, Turkey
[2]Department of Machine, Asim Kocabiyik Vocational School of Higher Education, Kocaeli University, Kocaeli, Turkey
[3,4]Department of Automotive Engineering, Faculty of Technology, Kocaeli University, Kocaeli, Turkey
[5]Department of Materials and Metallurgy, Faculty of Technology, Marmara University, Istanbul, Turkey
rsamur@marmara.edu.tr
*Corresponding author

Abstract

Friction stir welding (FSW) between 2 mm thickness AA 5754 aluminum alloy sheet was researched in the current research. The welded joints were qualified by its aspects, microstructural ,mechanical features and corrosion behavior at cell temperature. The effect of the conical tool geometry on the FSW AA5754 are investigated over potentiodynamic polarization, open circuit potential (OCP) monitoring, test of the susceptibility to corrosion, micro-hardness and tension tests. The thermo-mechanically affected zones adjacent to weld nugget are most susceptible to corrosion in the weld joints. Scanning electron microscopy (SEM) and energy dispersive spectroscopy (EDS) analyses on the stir zone suggested that, intermetallic phases of the base material were mechanically fractured, smeared and mixed to different geometries due to tool stirring. The increase in anodic reactivity in the weld zone was due to the sensitisation of the grain boundaries leading to intergranular attack. Enhancement of cathodic reactivity was also found in the nugget as a result of the precipitation of Mg-rich phases.

Keywords – AA5754 Aliminum, corrosion, friction stir welding

1 Introduction

In recent years, many industrial sectors such as automobile, aerospace etc. have shown their interest in the application of Friction stir welding FSW and also in understanding of the factors that result in defects in FSW joints . Defects such as tunneling defect and kissing-bond in FSW joints are quite different from conventional fusion welding flaws. Typically, FSW parameters such as tool design, tool rotation and traverse speed, depth of tool plunge, angle of tool tilt, tool pin offset and welding gap etc. may lead to the defect formation, if they are not selected properly. Specially during joining of dissimilar materials using FSW, the pin offset plays an important strategic role in influencing the weld quality. Selection of offset position is often tricky and decision on this is carefully taken based on the physical, mechanical, metallurgical and thermal properties of the two dissimilar materials being joined. Similarly, the magnitude of plunge depth also plays a vital role during plastic deformation at the time of stirring and consequently its value is also chosen carefully to obtain desired results [1].

The shape of this weld nugget approximates that of the tool cross-section,although the FSW process leads to an asymmetry between the two sides of the weld. On the advancing side of the weld, where the tool rotation is along the welding direction, the edge of the weld nugget is more apparent than the diffuse boundary on the retreating side, where the tool rotation is opposite the welding direction[**2**].

Because it is a solid state joining process that no melt metal emerges during welding,and can avoid many defects in fusion welding techniques,

Friction stir welding FSW has been used on many alloys that are typically difficult to be welded, many advantages of friction stir welding make Friction stir welding FSW extremely attractive for the joining of aerospace aluminum alloy and magnesium alloy [3].

The resulting microstructures of friction stir welds are described by the different zones as follows: 1) the base metal (BM), sometimes called the parent metal (PM) which is the material remote from the weld that has not been deformed, and is not affected by the heat in terms of microstructure or the mechanical properties; 2) the heat affected zone (HAZ) which is a region that lies closer to the weld centre and has experienced a thermal cycle that has modified the microstructure and/or the mechanical properties, however, no plastic deformation has occurred in this area;3) the thermo mechanically affected zone (TMAZ) which is a region where the FSW tool has plastically deformed the material at the weld interface; and 4) the weld nugget (WN) which is the fully recrystallized area, sometimes called the stir zone (SZ) or the stir nugget (SN), and refers to the zone previously occupied by the tool pin during FSW [4].

The stress corrosion cracking (SCC) behaviour of aluminium alloys has been studied for the past five decades and is still a research area of high interest due to the demand for higher strength aluminium alloys for fuel saving. This chapter brings out the general understanding of the SCC mechanism(s) and the critical metallurgical issues affecting the SCC behaviour of aluminium alloys. The developments made so far with regard to alloying and heat treatment of aluminium alloys for high SCC resistance are discussed. An overview of the available literature on the SCC of aluminium alloy weldments and aluminium alloy metal matrix composites is also presented [5].

Aluminum alloys (AA) exhibit low corrosion rate in chloride solutions. But they do suffer from pitting. The pitting resistance of AA depends on their purity. The 1xxx series (purest alloy) is more resistant than the other AA. Al–Mg alloys display good resistance against general and localized corrosion [6].

Aluminum crafts require less fuel. They are capable of high speed; and have increased load capacities, greater ease of recycling, and high anticorrosion properties. Ships constructed with

5000-series Al alloy suffer little corrosion in marine environments, with a coat of paint providing sufficient corrosion protection for the ship. However, considerable corrosion occurs at the welds, and problems exist with deformation due to the welding heat. Moreover, the mechanical strength near the welds is low [7].

Also pointed out the corrosion resistance of the welds, asserting that it is the real issue in dissimilar friction stir welding, due to a galvanic interaction between both welded alloys, and requires further investigations. Friction stir welding induces large plastic deformations and complex metal flows, leading to the stirring of both materials to be welded and, hence, to the formation of the weld itself. Some general observations concerning the metal flow in dissimilar friction stir welding are commonly accepted. have observed that the intercalation of lamellae of two alloys during welding creates complex vortex, whorl, and swirl features.Observed the presence of a lamellar material flow pattern due to the differential flow, suggesting material mechanical, but no chemical, mixing within the stirred zone [8].

The region between the nugget's thermomechanically heat-affected zone. Within this region, the coarsened precipitates control the corrosion behaviour. Thus, the main idea is to partially redissolve or reduce the dimensions of the coarse precipitates within the grain interior and along the grain boundaries. During the welding, the region along the nugget's thermomechanically heat-affected zones experiences a temperature between 250 and 450 °C for a period of minutes .Exposure to such temperatures causes a modification of the microchemistry and microstructure and a worsening of the corrosion properties, in particular of the zones adjacent to the weld nugget [9].

2. Experimental procedure

Alloys of the 5xxx series contain particles of Mg_2Al_3, Mg_2Si and intermetallic phases with chromium and manganese. Transport and is widely used in the automotive industry hardened and cold-deformation strength in the gain of 2 mm thickness with aluminum alloy 5754 (AlMg3) material is used. In friction stir welding, milling and conical geometry is used friction stir tool. Tool rotational speed of 1600 rev/min, the welding feed rate of 125 mm/min was kept constant. Get sheets in position, so that no gap between solid state welding technique by which friction stir welding method is applied to the combined one-sided butt welding [10].

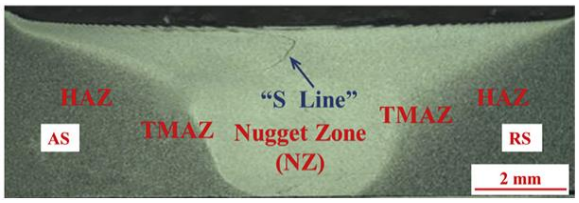

Fig.2.1. AA5754 Aluminum sheets welded by friction stir welding FSW (RS) retreating side and (AS) advancing side [11].

2.1. The design of the materials to be joined by friction stir welding

AA 5754 aluminum alloy sheet of 2 mm thick were used in this study. Chemical analysis of the material in material laboratories of the spectral analyzer (Figure 2.2) and Table 2.1 is given. AA 5754 mechanical properties of the material are indicated in Table 2.2, tensile test, the material test laboratory in Universal device, the micro-hardness Vickers hardness measurement is made on the device.

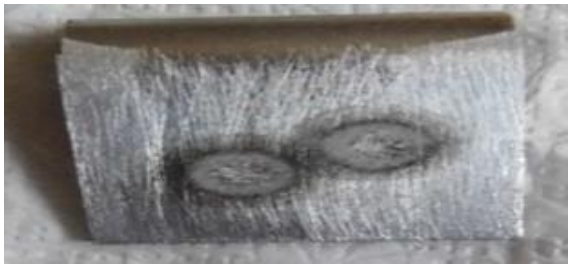

Fig 2.2 Determination of the chemical analysis by the spectral analyzer of the aluminum material used in the welding process.

Table 2.1 Chemical analysis of aluminum materials used in the welding process

Material	% Fe	% Si	%Cu	%Mn	% Mg	% Zn	%Ti	%Cr	%Al
AA5754	0,312	0,23	0,024	0,34	3,2	0,164	0,098	0,26	Remaining

Table 2.2 Mechanical properties of the aluminum material used in the welding process

Sample	Tensile Strength (N/mm^2)	% Elongation	Hardness (Hv)
AA 5754	232	15	76

2.2 The Design Of The Friction Stir Tool Material And Production

2.2.1 Friction Stir Tool: Friction stir welding welding tools, the hot-work tool steels are manufactured in lathe machining processing to manufacturing. Tools of conical tip (Figure 2.3,2.4). Chemical analysis of the stir tool materials, made of materials and laboratory results in Table 2.3 are given. Shown in Figure 2.3 tools made from hot work tool steel, heat treated during the manufacturing process and heat treatment applied after the material has reached a value of 58-60 HRC. The tool, the tool will pass the holder part to connect to the tool holder Ø16mm (Figure 2.4) in diameter, it was manufactured according to the manufacturing tolerances specified in the picture. A step was made to prevent the escape tool than the tool back. Tool shoulder, Ø20 (Figure 2.4) is based on the diameter of the tool includes a tool holder is prevented escape. Before the start of progress in the horizontal direction of movement of the stirrer tip, each welding operation in order to provide adequate heat input, the shoulder portion of the tool is made 50 seconds friction between the parts. Then, in accordance with parameters of the tool are given in Table.2.4 Rotational velocity and traverse speed.

Fig 2.3 48CrMo 6 7 It is made of hot work tool steel friction stir tools.

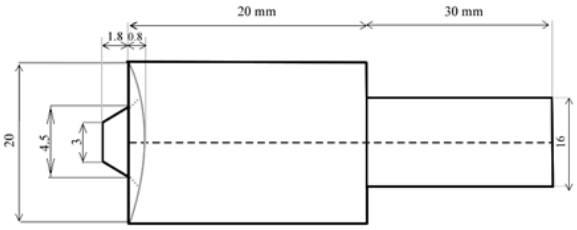

Fig 2.4 Friction stir welding tool technical drawing

Table 2.3 Friction stir welding tool (48CrMo67) (%) The chemical composition of hot work tool steels.

Chemical Analysis (SAE/AISI)								
C	Si	Mn	P	S	Cr	Mo	V	Fe
0,48	0,25	0,75	0,030	0,030	1,45	0,20	0.30	Remaining

Fig 2.5 The milling machine used for friction stir welding process. Welding is performed with fixed clamping shoe parts.

2.4 Selected welding parameters for the welding process

Table 2.4 Selected welding parameters for the welding process

Rotational velocity (rpm)	Traverse Speed (mm/min)	FSW connect the tools location	Sample Code
1600	125	Derived parts 2 ° angle	R1

Table 2.5 Tool profile and the experimental parameters used in friction stir welding

Material	Friction Stir Welding tool Profile	Rotational velocity (rpm)	Traverse Speed (mm/min)	Sample Code
AA 5754	Conical	1600	125	R1

2.5. Sample preparation for metallographic and mechanical tests

Tensile testing, materials change shape when the load is applied (elongation) and a measurement method to determine the failure analysis [12].

The weld surface, and the view taken from each sample was reverse displayed makrograf. Eye passing the examination, welded to a 5754 aluminum alloy of the plate, according to plans to be tested in accordance with TS test samples EN 288-3 standard and are not affected by the heat in the precise cutting device is cut using a water jet (Figure 2.6-2.9).

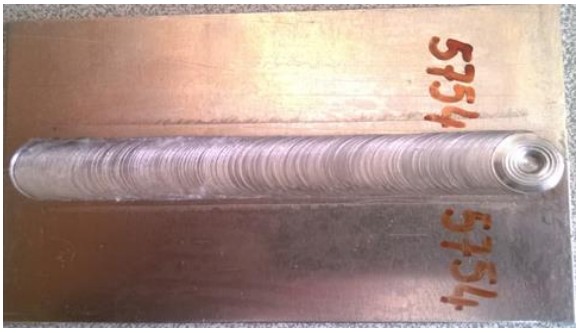

Fig 2.6 With friction stir welding method macrograph of accurate combined AA 5754 aluminum alloy sheet

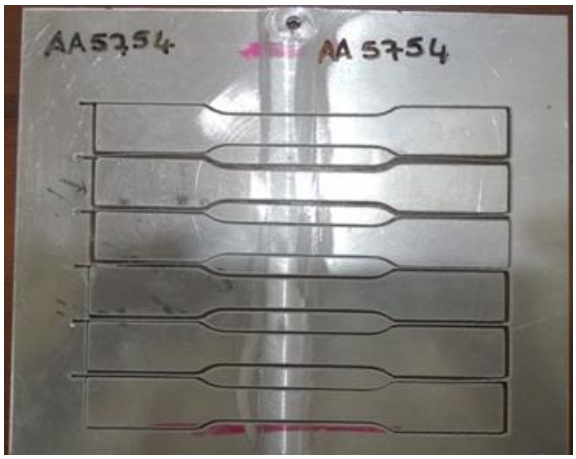

Fig 2.7 From welded sheets (ASTM E8M-04) cutting with a water jet of the appropriate standard tensile samples [13].

Fig 2.8 Front view of the water jet cutting part of the extrusion according to the ASTM standard test sample of the welded sheet [13].

Fig 2.9 Reverse view of the water jet cutting part of the extrusion according to the ASTM standard test sample of the welded sheet [13].

2.6 Macrostructure and microstructure examination

Macrostructure and microstructure examination image analyzer mounted on a light microscope was used for. Scanning electron microscopy (SEM) examination EDS structure for the combined scanning electron microscopy

(Electron Dispersive Spectroscopy) is used. 2mm thick section of welded parts after hot forming step sanding and polishing machines in the mesh up to 1200 and 1'm like polished with diamond paste is prepared. Keller in etching reagent (95 ml water, 1 ml HF, 1.5 ml HCl and 2.5 ml HNO3) was used [14].

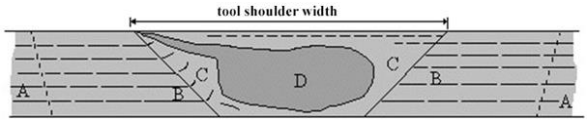

Fig. 2.10. Schematic representation of the microstructure of the friction stir welding of aluminum alloy AA5754 made. A: The base material (BM), B: heat affected zone (HAZ), C: thermo mechanical affected zones (TMAZ), D: dynamically recrystallized zone (SZ) (NZ) (WN) [15].

Fig 2.11. Mounting friction stir welded sample was obtained and cross-sectional sample of Mountains.

Fig 2.12 Friction stir welding of AA5754 aluminum combined with a try in the microstructure of the sample section (a: base metals, b: the area under the heat effect, c: thermo mechanical affected zone and nugget zone: core [14].

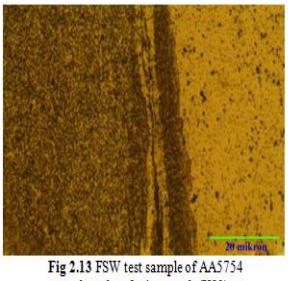

Fig 2.13 FSW test sample of AA5754 a, b and c of micrograph (X50)

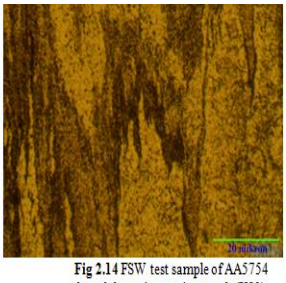

Fig 2.14 FSW test sample of AA5754 b and the region c micrograph (X50)

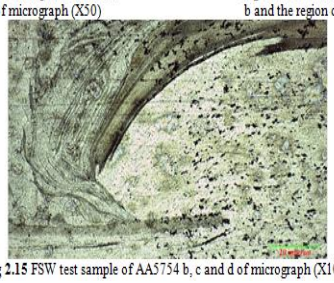

Fig 2.15 FSW test sample of AA5754 b, c and d of micrograph (X100)

2.7 Microhardness Testing Results and Analysis

Welded plate heat is not affected from the welded parts for hardness measurements sample are cut with water jets. Passing through metallographic procedures were performed after the hot molding process to the diamond polishing paste level. Vickers microhardness tester was used for hardness measurements. Hardness measurements in the 2mm thick plates for welded parts in cross-section in the hot forming, grinding, polishing and etching are applied. Hardness measurements were used 200 g load and 10 s. Microhardness measurements supply section axis direction by 0.5 mm at the top, middle and bottom axis is applied to the section (Figure 2.16).

Fig 2.16 Microhardness measurement was made of the origin of the upper, middle and lower schematic representation of linear axis [16].

Welded connections (Figure 2.16) from the correct base metal applied linear micro hardness measurement results from the merger of three separate centers are given in table 2.6. When the hardness profile examination, the hardness of the weld metal, base metal has increased in all the samples correctly. Hardness was slightly increased in the regions recrystallize in the welding center. NZ re-crystallized welding center, it is possible to connect to shrinkage of the increase in the value of recrystallized grains hardness. The fall in the value of TMAZ and HAZ hardness in the region is possible to connect to the presence of grain coarsening and micro space.

Table 2.6 Hardness values are taken from the Welding cross-section

Distance from Welding center (mm)	Hv_{200} The Vertical Axis	Hv_{200} Central Axis	Hv_{200} Bottom Axis
-20	75	75	75
-18	74	71	70
-16	70	70	69
-14	68	71	68
-12	66	70	68
-10	64	70	64
-8	62	64	62
-6	61	63	64
-4	61	61	67
-2	63	64	68
0	65	65	68
2	66	64	69
4	67	60	65
6	65	61	65
8	68	59	68
10	70	66	72
12	73	68	71
14	75	73	74
16	77	76	75
18	76	77	75
20	75	80	76

Table 2.7 The tool with the friction stir welding method 1600 rev/min rotation and 125 mm/ min with a feed rate of the welded plates created (ASTM E8M-04) cut to the appropriate standard tensile stress-strain results obtained from samples

Sample Code	Rotational velocity (rpm)	Traverse Speed (mm/min)	Average Tensile Strength (N/mm^2)	Elongation %	Evaluation
AA5754 R1	1600	125	196,26	14,5	Samples Were Damaged in TMAZ
AA5754 R1		125	190,9	10,8	Samples Were Damaged in TMAZ
AA5754 R1		125	189,95	11,76	Samples Were Damaged in TMAZ
	Average	125	192.37	12.35	

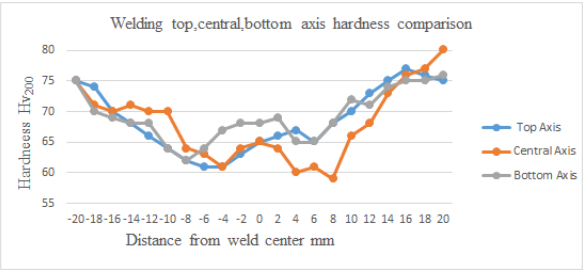

Fig 2.17 1600 rev/min rotation and 125 mm/min feed rate to the top of the line joining the welding made from the cross-sectional area, a graphical representation of the upper, middle and lower axis.

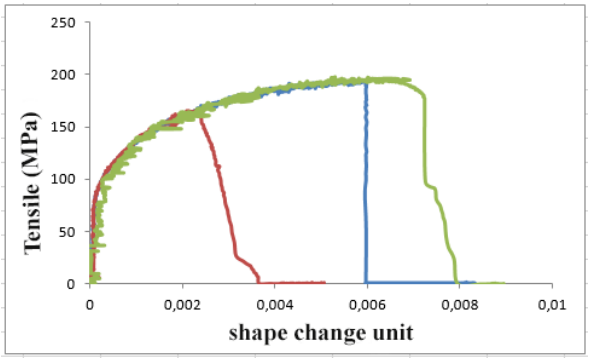

Fig 2.18 Friction stir welding of the lead with 1600 rev/min rotation and 125 mm/min advance speed of the welded sheet formed (ASTM E8M-04) obtained according to standard tensile samples cut from the stress-strain graph.

Fig 2.19 Tensile specimen after fracture; the FSW accomplished at tool rotational velocity of 1600 rpm, tool traverse speed of 125 mm/min (ASTM E8M-04).

2.8 The tool with the friction stir welding method 1600 rev/min rotation and 125 mm/min with a feed rate of the welded plates created (ASTM E8M-04) obtained from samples cut tensile stress-strain analysis according to standards

When the macro photo surface, flat and smooth surface that take place any sources of error seems to be obtained (Figure 2.6,2.7,2.8,2.9). Figure 2.18 at 125 mm / min table feed source combined with parameters coded R1 is seen drawing curves of welded joints. R1 coded true stress-strain curve of the welded sample is given in Figure 2.18.Tensile test results of samples (TMAZ) ductile damage occurring species in the region are shown in Figure 2.19. When the light microscope micrograph taken through the weld in Figure 2.13,2.14,2.15 are examined, it is seen that there are any gaps on the surface and unconnected areas.R1 coded tensile pull test samples stored in the sample-elongation values are given in Table 2.7. Tensile strength and elongation values when analyzed average 192.37 N / mm^2 is clear that the numerical values exhibited ductile behavior. 2.13,2.14,2.15 the mixing zone as shown in Figure (d) is fine-grained structure with small thermo-

mechanically affected zone (b, c) is composed of more coarse and recrystallization rated one. Constant 1600 rev / min rotation and 125 mm / min table feed rate using the combined R1 coded fracture surfaces of samples are examined, it is again the crystallization, the grain coarsening and the micro-cavities (TMAZ) rupture zones have occurred (Figure 2.19).As it is shown in Figure 2.13,2.14,2.15 (a, b, c) source zones and the thermo-mechanically affected zone (TMAZ) transition area between the observed markedly. In micrographs obtained by light microscopy it was determined that forming void of amalgamation of limits on AA5754 aluminum.The welded specimens were produced by employing a constant tool traverse speed of 125 mm/min and rotating speed of 1600 rpm yielded a maximum tensile strength of 196 MPa which was 84% of the base material strength.

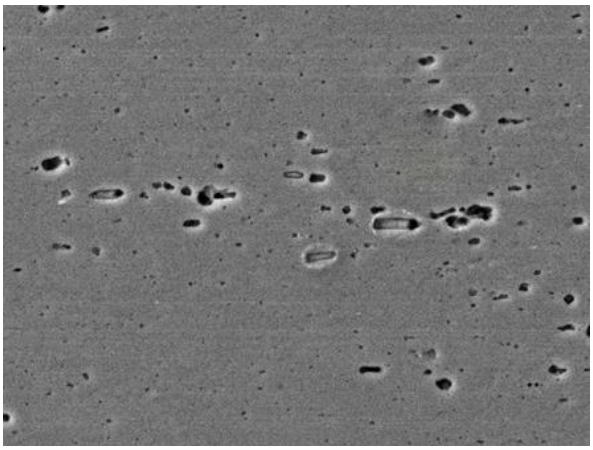

Fig.2.20 Scanning electron micrographs obtained from AA5754 base Metal (BM).

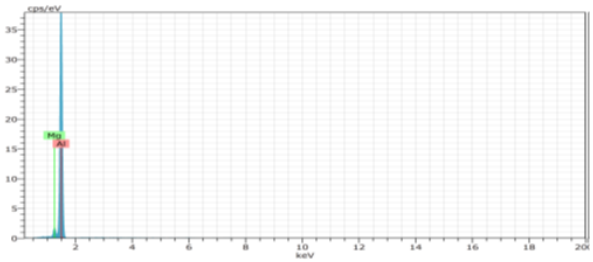

Fig.2.21 Scanning electron microscope (SEM) EDS spectrum of AA5754 Base metal (BM).

Table 2.8 Chemical composition of AA5754 Base metal(BM)

Element Series	C norm. [wt.%]	C Atom. [wt.%]	C Error [at.%]	(1 Sigma) [wt.%]
Aluminum K-series	106.61	96.72	96.37	5.14
Magnesium K-series	3.62	3.28	3.63	0.25
Total	110.22	100.00	100.00	5.39

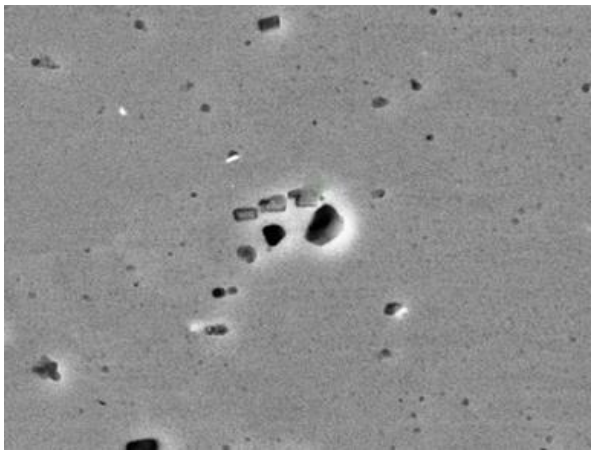

Fig.2.22 Scanning electron micrograph image in the HAZ, TMAZ and SZ of friction stir weld of AA5754 alloys showing recrystallized grains with re-precipitated intermetallic different in size and distribution compared with the intermetallic in the parent metals.

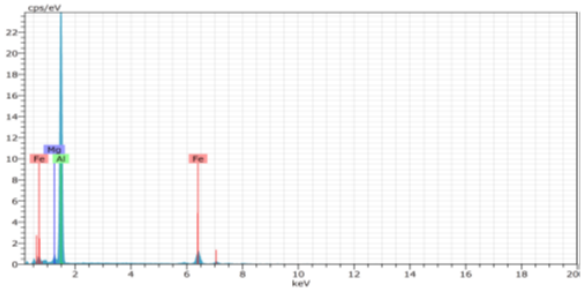

Fig.2.23 Scanning electron microscope (SEM) in EDS spectrum of the HAZ, TMAZ and SZ.

Table 2.9 Chemical composition of in the TMAZ and SZ

Element Series unn.	C norm. [wt.%]	C Atom. [wt.%]	C Error [at.%]	(1 Sigma) [wt.%]
Iron K-series	19.02	19.64	10.54	0.63
Aluminum K-series	76.00	78.48	87.15	3.69
Magnesium K-series	1.81	1.87	2.31	0.16
Total:	96.84	100.00	100.00	

2.9 Corrosıon Measurement of FSWed AA5754 Aluminium Alloy Sheets

Galvanostat / potentiostat (Gamry model PC4/300) was used for corrosion test. A three-electrode system was employed which was

composed of a counter electrode of carbon rod, a reference electrode of saturated calomel electrode (SCE) and a work electrode of tested sample (square cube shape samples with an average size of 2 mm x 2 mm). During electrochemical corrosion test, the electrode potential was scanned at a scan rate of 1 mV/min from -1000 mV towards anodic potential and the corrosion current values were recorded in 1 mV steps for both anodic and cathodic polarization in the unit of A/cm^2 by dividing the current values of the each sample by their initial total surface area (Figure 2.24).

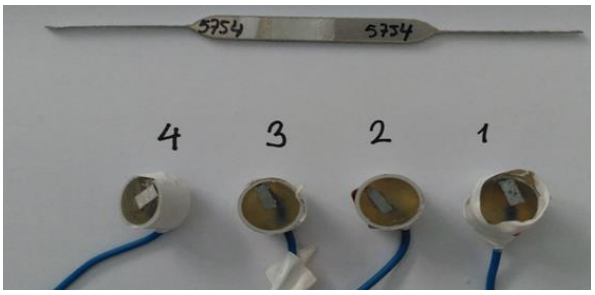

Fig.2.24 Potentiodynamic polarization and Variation of the open circuit potential with time of FSWed AA5754 Corrosion measurement samples 1- Parent/Base Metal(PM)(BM) 2-Heat affected zone (HAZ) 3- Thermo mechanically affected zone (TMAZ) 4- stir zone (SZ) or the stir nugget (SN) or weld nugget (WN).

Fig. 2.26 shows the potentiodynamic polarization curves of base metal, HAZ, TMAZ and nugget zones. As shown in Fig. 2.26, there is obvious difference between base metal and other zones, but HAZ, TMAZ and nugget zones show similar polarization behavior. The corrosion potential of HAZ zone is higher than that of TMAZ and nugget zones. Table 2.10 presents the average electrochemical parameters calculated for the zones of the friction stir weld according to ASTM G102. It is obvious that the corrosion potential (E_{corr}) of HAZ zone (-771 mV) is superior to those of TMAZ zone (-797 mV) and nugget zone (-908 mV), and the result of corrosion current (I_{corr}) indicates that HAZ zone (927 x 10^{-9} A/cm^2) is more resistant to corrosion than TMAZ zone (12700 x 10^{-9} A/cm^2) and nugget zone (128000 x 10^{-9} A/cm^2). According to the electrochemical results listed in the Table 2.10, HAZ zone exhibits excellent anticorrosion properties over TMAZ and nugget zones.

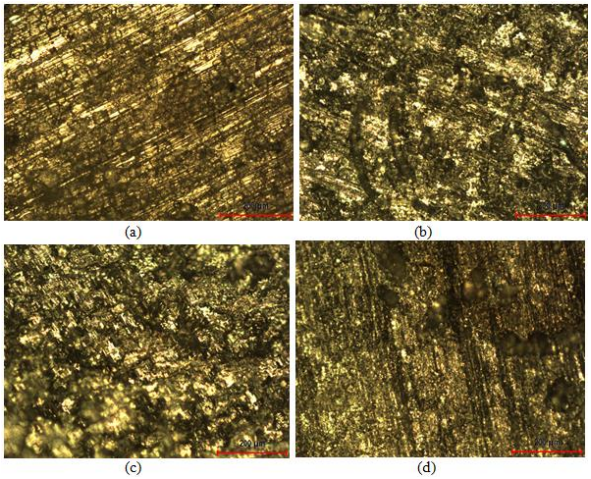

Fig. 2.25 Surfaces of corroded (a) base metal, (b) HAZ, (c) TMAZ and (d) nugget zones.

Table 2.10 Average electrochemical parameters of base metal, HAZ, TMAZ and nugget zones.

Conditions	I_{corr} (x 10^{-9} A/cm^2)	E_{corr} (mV)
Base Metal	0,0885	-863
HAZ zone	927	-771
TMAZ zone	12700	-797
Nugget zone	128000	-908

Figure 2.25 shows the surface micrographs of base metal, HAZ, TMAZ and nugget zones after corrosion test. It was noted that roughness of the corroded sample surface had been increased by closing to nugget zone. Corrosion had occurred by dissolution of the matrix and intermetallic phase. Since higher amount of heat in the friction stir weld leads to increase in the number of defect, corrosion rate is also expected to increase due to galvanic coupling.

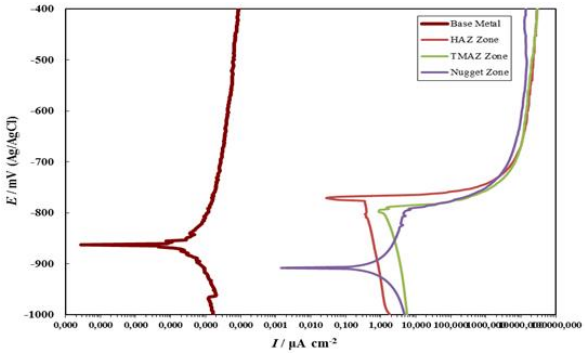

Fig.2.26 Potentiodynamic polarization curves of FSWed AA5754 Corrosion measurement of Base Metal (BM), Heat affected zone (HAZ),Thermo mechanically affected zone (TMAZ), stir nugget (SN).

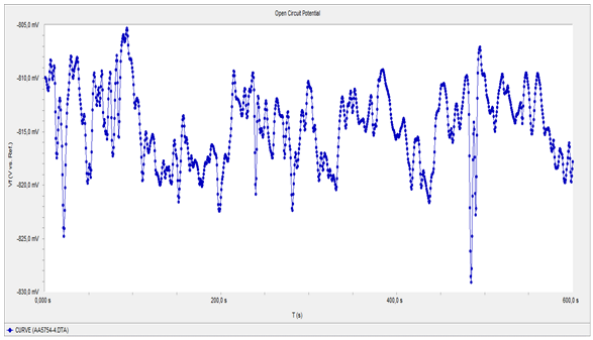

Fig.2.27 Variation of the open circuit potential with time.OCP measurement of Parent metal (BM).

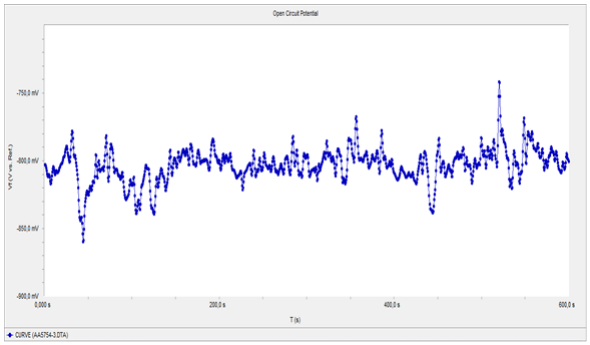

Fig.2.28 Variation of the open circuit potential with time.OCP measurement of Heat heat affected zone (HAZ) zone.

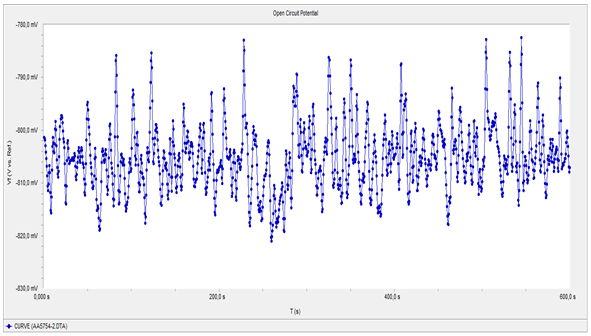

Fig.2.29 Variation of the open circuit potential with time.OCP measurement of (TMAZ) zone.

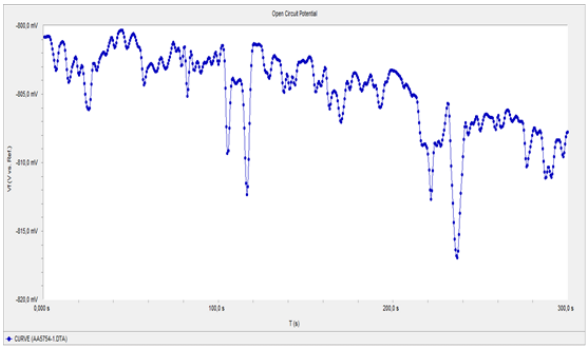

Fig.2.30 Variation of the open circuit potential with time.OCP measurement of (SZ)(NZ) zone.

3 Conclusions

a. AA 5754 pre-designed aluminum alloy 1600 rev/min constant speed of 125 mm/min with friction stir welding parameters, the following are the results obtained in the friction stir welded to be taken unilaterally. Friction stir welding in the butt welded parts is melting less heat input welding method according to the deformation has not occurred (figure 2.6-2.9).

b. Friction stir welding applications, due to less burr tool will be seated on the shoulder of the plate very well.

c. The micrographs obtained with the light microscope, it was determined that the merger creates clear boundaries in the region of AA5754 aluminum (Figure 2.13 to 2.15).

d. Welded AA5754 tensile strength of the material has dropped by around 30% compared to the tensile strength of the weld-base material.

e. The weld seam; top, mainly from the middle and lower axis linear stiffness values taken from the welding center regularly has been shown to increase towards the metal.

f. Metallic materials due to a temperature increase before the heat recovery and then recrystallization, grain growth is a classic case of being in the next step. welding process, the tool's 1600 rev/min to reach rotational speeds with high tensile strength of the weld is determined in the micrograph is formed in the recrystallization of the welding process (Figure 2:13 to 2:15).

g. Scanning electron microscopy (SEM) and energy dispersive spectroscopy (EDS) analyses on the stir zone suggested that, intermetallic phases of the base material were mechanically fractured, smeared and mixed to different geometries due to tool stirring.

h. It is obvious that the corrosion potential (Ecorr) of HAZ zone (-771 mV) is superior to those of TMAZ zone (-797 mV) and nugget zone (-908 mV), and the result of corrosion current (Icorr) indicates that HAZ zone (927 x 10^{-9} A/cm^2) is more resistant to corrosion than TMAZ zone (12700 x 10^{-9} A/cm2) and nugget zone (128000 x 10^{-9} A/cm2). According to the electrochemical

results listed in the Table 2.10, HAZ zone exhibits excellent anticorrosion properties over TMAZ and nugget zones.

4 Acknowledgements

Asst.Prof.Dr.SAMUR acknowledges the support by Marmara University, Scientific Research Projects Department(BAPKO),Projects FEN-D-110815-0396 and FEN-C-YLP-030114-0014.The authors also acknowledge the SEM operator Mr.Semih ÖZBEY of Department of Materials and Metallurgy, Faculty of Technology, Marmara University.

Note: The responsible translator for English language is O. Faruk CANTEKİN, School of Foreign Languages, Gazi University, Turkey

5 References

[**1**] Khan, N.Z.; Siddiquee, A.N.; Khan, Z.A.; Shihab, S.K. Investigations on tunneling and kissing bond defects in FSW joints for dissimilar aluminum alloys. Journal of Alloys and Compounds. 2015; 648, 360-367.

[**2**] Fonda, R.W.; Pao, P.S.; Jones, H.N.; Feng, C.R. Microstructure, mechanical properties, and corrosion of friction stir welded Al 5456. Materials Science and Engineering A. 2009; 519, 1–8.

[3] Shen, C.; Zhang, J.; Ge, J. Microstructures and lectrochemical behaviors of the friction stir welding dissimilar weld. Journal of Environmental Sciences 2011; 23, 32–S35.

[4] Threadgill, P L. Terminology in friction stir welding. Science and Technology of Welding and Joining, 2007; 12(4), 357–360.

[5] Kannan, M.B.; Srinivasan, P.B.; Raja, V.S. Stress corrosion cracking (SCC). A volume in Woodhead Publishing Series in Metals and Surface Engineering 2011; 307–340.

[6] Kalita, S.J. Microstructure and corrosion properties of diode laser melted friction stir weld of aluminum alloy 2024 T351. Applied Surface Science. 2011; 257, 3985–3997.

[7] Park, S.H. Corrosion and optimum corrosion protection potential of friction stir welded 5083-O Al alloy for leisure ship. Trans. Nonferrous Met. Soc. China. 2009; 19, 898-903.

[8] Jonckheere, C.; de Meester, B.; Denquin, A.; Simar, A. Torque, temperature and hardening precipitation evolution in dissimilar friction stir welds between 6061-T6 and 2014-T6 aluminum alloys. Journal of Materials Processing Technology. 2013; 213, 826– 837.

[9] Paglia, C.S.; Buchheit, R.G. A look in the corrosion of aluminum alloy friction stir welds. Scripta Materialia. 2008; 58, 383–387.

[10] Steuwer, A.; Peel, M. J.; Withers, P.J. Dissimilar Friction Stir Welds in AA5083–AA6082: The Effect of Process Parameters on Residual Stress. Materials Science and Engineering A. 2006; 441, 187–196.

[11] Wang, Q., Zhao, Y.; Yan, K.; Lu, S. Corrosion behavior of spray formed 7055 aluminum alloy joint welded by underwater friction stir welding. Materials and Design. 2015; 68, 97–103.

[12] Sato, Y.S.; Kurihara, Y.; Park, S.H.C.; Kokawa, H.; Tsuji, N. Friction Stir Welding Of Ultrafine Grained Al Alloy 1100 Produced by Accumulative Rollbonding. Scripta Materialia. 2004; 50, 57-60.

[13] Elangovan, K.; Balasubramanian, V. Influences of tool pin profile and welding speed on the formation of friction stir processing zone in AA2219 aluminium alloy. Journal of Materials Processing Technology, 2000; 200, 163–175.

[14] Doğan, S. AA 5754-H22, Alüminyum Alaşımının Sürtünme Karıştırma Kaynağında İşlem Parametrelerinin Mikroyapı Ve Mekanik Özelliklere Etkileri, Yüksek Lisans Tezi, Metalürji Mühendisliği Anabilim Dalı, Osmangazi Üniversitesi Fen Bilimleri Enstitüsü, Ekim 2006.

[15] Bradley, G.R.; Jones, M.N. Geometry and Microstructure of metal inert gas and friction stir welded Aluminium Alloy. 2000; 5383-H321, 86p.

[16] Şık, A.; Ertürk, İ.; Önder, M., AA2024 Alüminyum Alaşımının Sürtünme Karıştırma Kaynağında Farklı Parametrelerin Mekanik Özelliklere Etkisinin İncelenmesi, Pamukkale Üniversitesi Mühendislik Bilimleri Dergisi. 2010, 16(2), 139-147.